Electrocarboxylation Reactions

Rotating Ring-Disk Electrode, Voltammetric, and Electron Spin Resonance Studies of Dialkyl Fumarates and Maleates

Lun-Shu R. Yeh* and Allen J. Bard**

Department of Chemistry, The University of Texas at Austin, Austin, Texas 78712

ABSTRACT

The reduction of the diactivated olefins dimethyl fumarate (DMeF), diethyl fumarate (DEF), di-n-butyl fumarate (DBF), dimethyl maleate (DMM), diethyl maleate (DEM), and di-n-butyl maleate (DBM), in N,N-dimethylformamide-tetra-n-butylammonium iodide solutions saturated with dissolved carbon dioxide at a platinum electrode has been studied by rotating ring-disk electrode and cyclic voltammetry and *in situ* electron spin resonance spectroscopy. The results indicate that the rate-determining step for each compound is the reaction of the radical anion with CO_2; the radical anions are also involved in the dimerization and (for maleates) isomerization reactions which occur in the absence of CO_2. The coupling of the carboxylated radical to dimeric carboxylate is rapid. The rate constants for the reaction of the radical anions with CO_2 were faster for maleates than for fumarates; pseudo-first order rate constants for a saturated CO_2 solution (*ca.* 0.2*M*) are DMeF, 1.5 sec^{-1}; DEF, 0.47 sec^{-1}; DBF, 0.35 sec^{-1}; DMM, 32.0 sec^{-1}; DEM, 19.4 sec^{-1}; and DBM, 18.0 sec^{-1}.

There have been numerous studies of the reactions of electrogenerated radical anions of diactivated olefins (1-12). Hydrodimers are the major product for reductions in aprotic solvents such as N,N-dimethylformamide (DMF), formed by coupling of radical anions followed by protonation. Thus for dialkyl fumarates (abbreviated throughout as F) the reaction sequence is

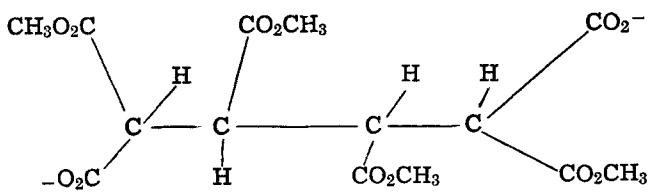

1 or $^{-}O_2CDCO_2^{-}$

$$F + e \rightarrow F^{\cdot -} \quad [1]$$

$$2F^{\cdot -} \xrightarrow{k_{2F}} D^{2-} \quad [2]$$

Recent studies (12, 13) show that the *cis*-forms (maleates or M) follow a similar reaction scheme

$$M + e \rightarrow M^{\cdot -} \quad [3]$$

$$2M^{\cdot -} \xrightarrow{k_{2M}} D^{2-} \quad [4]$$

but that the coupling rate for the radical anions derived from the maleates is about 2000 times that of the fumarate anions. Moreover, isomerization of $M^{\cdot -}$ also occurs

$$M^{\cdot -} \xrightarrow{k_1} F^{\cdot -} \quad [5]$$

Cross-coupling between $M^{\cdot -}$ and $F^{\cdot -}$ is also possible, but this rate is apparently slow compared to the reaction of two $M^{\cdot -}$'s (12).

Carbon dioxide has been shown to react with organic anionic intermediates generated electrochemically in aprotic media (14-17). Recently, Tyssee and Baizer (18, 19) studied the reduction of diactivated olefins in the presence of CO_2. For dimethyl maleate (DMM), production of the carboxylated dimer (**1**), 1,2,3,4-tetramethyl-1,1,2,3,4,4-butanehexacarboxylate, was demonstrated. These authors suggested

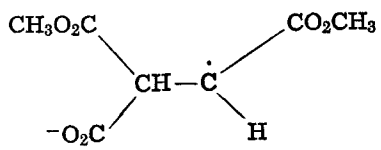

2 or $MCO_2^{\cdot -}$

two possible reaction paths leading to **1**: dimerization of $M^{\cdot -}$, [4], followed by reaction with CO_2

$$D^{2-} + 2CO_2 \rightarrow {}^{-}O_2CDCO_2^{-} \quad [6]$$

or reaction of $M^{\cdot -}$ with CO_2 to form the carboxylated radical anion (**2**) followed by dimerization

$$M^{\cdot -} + CO_2 \xrightarrow{k_M} MCO_2^{\cdot -} \quad [7]$$

$$2MCO_2^{\cdot -} \rightarrow {}^{-}O_2CDCO_2^{-} \quad [8]$$

An alternate path would involve coupling of $MCO_2^{\cdot -}$ with M followed by reduction and carboxylation, but the independence of yield of **1** with initial concentration of maleate makes this route less likely (19). An additional reaction path involves the ECEC sequence, [3], [7], followed by further reduction of **2**

$$MCO_2^{\cdot -} + e \rightarrow MCO_2^{2-} \quad [9]$$

$$MCO_2^{2-} + CO_2 \rightarrow {}^{-}O_2CMCO_2^{-} \quad [10]$$

3

where **3** is 1,2-dimethyl 1,1,2,2-ethanetetracarboxylate (18). The reduction in [9] occurs at somewhat more negative potentials than that in [3], so that this path is not significant at potentials of the first reduction wave.

In the work described here, the rate constants for the reaction of the radical anions with CO_2 were determined and the reaction paths of the carboxylated intermediates investigated. The reaction scheme for the maleates is quite complicated, since the rather rapid coupling and isomerization reactions [(for DMM, k_{2M}

* Electrochemical Society Student Member.
** Electrochemical Society Active Member.
Key words: reductive coupling, rotating disk electrode, *cis-trans*-isomerization, carboxylation.

$= 1.9 \times 10^5\ M^{-1}\ sec^{-1}$ and $k_1 = 2.2\ sec^{-1}$ (12)] occur in addition to the carboxylation reactions. The fumarates have a slower coupling reaction, and diethyl fumarate (DEF) and di-n-butyl fumarate (DBF) show no appreciable coupling on the RRDE time scale [for DEF and DBF, $k_{2F} = 44\ M^{-1}\ sec^{-1}$ and $25\ M^{-1}\ sec^{-1}$, respectively (5)]. Thus in the absence of CO_2 both DEF and DBF show the theoretical collection efficiency, N, for generation of radical anions at the disk and collection at the ring electrode. Here, changes in the collection efficiency upon addition of CO_2 for different concentrations of DEF and DBF can be used to study the reaction of $F^{\cdot -}$ and CO_2. The study was also extended to the maleates, taking account of their inherent reactions using rate constants determined previously (12), so that a comparison of the reactivity of the radical anions derived from the *cis-* and *trans-* forms of the same species could be made.

Experimental

The reagents, purification schemes, apparatus, and techniques were the same as those previously described (12). The CO_2 was instrument grade 99.99% from Big Three Industries, Incorporated. The RRDE with platinum disk and ring electrodes, constructed by Pine Instrument Company (Grove City, Pennsylvania), had $r_1 = 0.187$ cm, $r_2 = 0.200$ cm, and $r_3 = 0.332$ cm with a collection efficiency of 0.555.

In carboxylation experiments, CO_2 was bubbled through the solution for at least 30 min before the trials, and CO_2 was passed over the solution surface during the experiments. The cell was as used previously (12) with a Pt wire spiral auxiliary electrode in a separate compartment and a silver wire pseudo-reference electrode (Ag RE) also in a separate chamber connected to the RRDE chamber by sintered-glass disks. The electron spin resonance (ESR) measurements, carried out with a Varian Associates (Palo Alto, California) Model E-9 spectrometer at 100 kHz field modulation, followed the usual arrangement for *intra muros* electrochemical methods (20) with a Varian electrolytic cell accessory. The electrolysis current was maintained at a low level so that the working electrode potential was at the foot of the first reduction wave. Nitrogen was continually being bubbled in the solution reservoir before and during the experiments when they were conducted in the absence of CO_2. The flat cell was flushed with nitrogen before oxygen-free solution containing DMF, TBAI, and sample was introduced into it. The same solution in the reservoir was then continually bubbled with CO_2 before and during the experiments involving reactions with CO_2. The flat cell compartment was then flushed with an excess amount of CO_2-saturated solution to rinse it before a new experiment was conducted.

The concentration of dissolved CO_2 in the 0.1*M* TBAI-DMF solution was determined by adding 13 ml of 0.1*M* TBAI-DMF solution to a 25 ml volumetric flask followed by the placement of loosely packed glass fiber in the neck of the flask. CO_2 was slowly bubbled through this solution for 20 min and an increase in weight of 115 mg was observed. This corresponds to 0.2*M* dissolved CO_2 in the solution at room temperature (*ca.* 24°C) (neglecting any loss of DMF); the literature value for pure DMF at 20°C is 0.228*M* (21).

Results and Discussion

Dimethyl fumarate (DMeF), Diethyl fumarate (DEF), and Di-n-butyl fumarate (DBF).—Cyclic voltammograms for 0.1*M* TBAI-DMF solutions of DEF in the absence and presence of CO_2 are given in Fig. 1; the results for DMeF and DBF are very similar. The large decrease in the reversal anodic peak height indicates the consumption of $F^{\cdot -}$ by CO_2. The cathodic peak height does not change upon addition of CO_2, showing that the ECE route leading to **3** is not significant on this time scale (at these potentials). No additional oxidation peaks were observed suggesting that the $FCO_2^{\cdot -}$ formed is rapidly consumed in a following reaction.

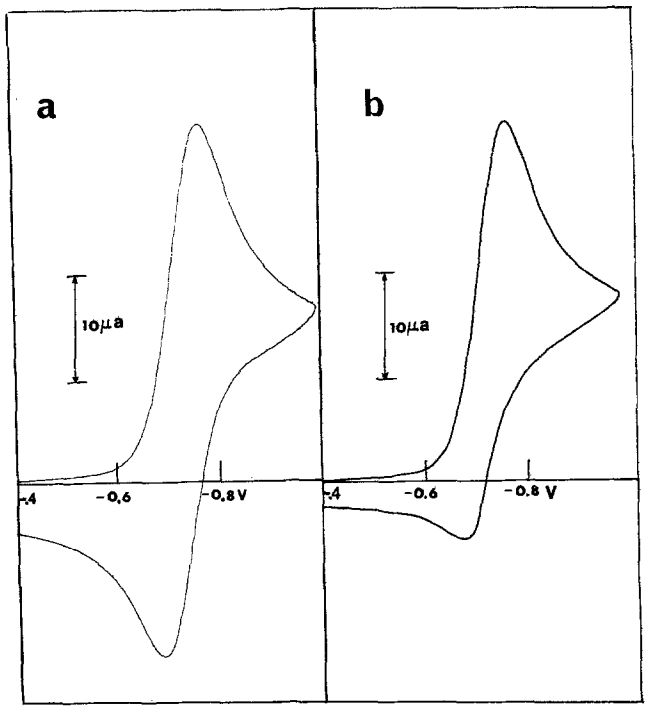

Fig. 1. Cyclic voltammograms (v = 100 mV/sec) of 0.1M TBAI-DMF solutions of 1.22 mM diethyl fumarate (a) without and (b) saturated with CO_2.

Rotating disk electrode (RDE) voltammograms (i_d *vs.* E_d) taken in the absence of CO_2 for millimolar solutions of DMeF and DEF exhibit a reduction wave at $E_{1/2} = -0.75$V *vs.* Ag-RE followed by a dip (at *ca.* -1.60V) in i_d after development of a well-defined plateau (22,23). This dip develops into a second reduction wave on addition of water or acid. In the presence of CO_2, the reduction potential of the first wave of these compounds shifted slightly (10-20 mV) to less negative potentials and the dip disappeared. This disappearance can be attributed to the reaction of F^{2-} with CO_2 thus decreasing the extent of the F^{2-}/F reaction which produces the dip (22). This effect was not investigated further and the discussion here is limited to processes occurring at the first reduction wave. Typical RDE data for the fumarates and values of the Levich constant $i_{d,l}/\omega^{1/2}C$ (where $i_{d,l}$ is the limiting disk current, ω is the angular velocity, and C the concentration) are given in Table I. For DBF this constant is essentially independent of ω and C. For DEF and DMeF a slight decrease in the Levich constant with increasing C is observed, perhaps caused by a small contribution of polymerization reaction consuming parent material. To obtain information about the rate of the $F^{\cdot -}/CO_2$ reaction and the mechanism of the reaction, RRDE experiments were undertaken, and the variation of the kinetic collection efficiency, N_k, expressed as the ratio of the ring current, i_r, to the disk current, i_d

$$N_k = |i_r/i_d| \qquad [11]$$

as a function of the disk current parameter *CONI* (4), where

$$CONI = |i_d/i_{d,l}| \qquad [12]$$

at different values of ω and C was determined. These N_k values were compared to working curves obtained by digital simulation (24) assuming the following reaction

$$F^{\cdot -} + CO_2 \xrightarrow{k_F} FCO_2^{\cdot -} \qquad [13]$$

Table I. Typical rotating disk electrode data for the first reduction waves in DMF-0.1M TBAI solutions in the presence of saturated CO_2

Concentration, C (mM)	Rotational rate ω (sec^{-1})	Limiting disk current $i_{d,1}$ (μA)	$i_{d,1}/\omega^{1/2}C$
	A. Dimethyl fumarate		
1.83	157	169	7.37
	207	194	7.37
	257	218	7.43
2.44	109	183	7.18
	157	222	7.26
	207	258	7.34
	257	288	7.36
3.56	109	256	6.88
	157	313	7.02
	207	360	7.03
	257	398	6.97
5.09	109	345	6.50
	157	418	6.55
	207	474	6.48
	257	528	6.48
	B. Diethyl fumarate		
1.82	109	107	5.63
	157	130	5.70
	207	148	5.65
2.43	109	142	5.60
	157	172	5.65
	207	196	5.60
	257	218	5.60
3.65	109	210	5.51
	157	252	5.51
	207	292	5.56
	257	320	5.47
4.87	109	278	5.47
	157	334	5.47
	207	378	5.39
	257	420	5.38
6.10	109	348	5.46
	157	416	5.44
	207	487	5.55
	257	536	5.48
	C. Di-n-butyl fumarate		
1.54	109	75.6	4.70
	157	92.0	4.77
	207	105	4.74
	257	118	4.78
2.20	109	110	4.79
	157	132	4.79
	207	154	4.86
	257	172	4.88
3.3	109	160	4.64
	157	196	4.74
	207	225	4.74
	257	254	4.80
4.4	109	218	4.75
	157	266	4.82
	207	305	4.82
	257	332	4.71
5.9	109	290	4.71
	157	357	4.83
	207	406	4.78
	257	458	4.84
7.7	109	380	4.73
	157	458	4.75
	207	528	4.77
	257	583	4.72
	D. Dimethyl maleate		
0.52	157	47.7	7.32
	207	54.4	7.27
1.05	157	95.1	7.23
	207	108	7.16
2.10	109	157	7.15
	157	186	7.08
3.15	109	227	6.90
	157	271	6.87
4.20	109	302	6.88
	157	362	6.88
	E. Diethyl maleate		
1.24	157	95	6.10
	207	108	6.06
	257	121	6.09
1.86	157	141	6.05
	207	161	6.02
	257	179	6.02
2.48	157	181	5.82
	207	208	5.82
	257	231	5.80
3.72	157	251	5.40
	207	288	5.39
	F. Di-n-butyl maleate		
1.10	157	72	5.22
	207	82	5.18
	257	92	5.21
1.54	157	99	5.14
	207	114	5.15
	257	126	5.11
2.42	207	178	5.10
	257	193	4.98

was rate determining. This reaction can be considered as a pseudo-first-order one, since the concentration of CO_2 in a saturated solution is 50-100 times that of the $F^{\cdot-}$. As in previous studies (4, 24), the dimensionless kinetic parameters XKT (first-order reactions) and $XKTC$ (second-order reactions), defined as

$$XKT = (0.51)^{-2/3}\nu^{1/3}D^{-1/3}\omega^{-1}k_1 \quad [14]$$

$$XKTC = (0.51)^{-2/3}\nu^{1/3}D^{-1/3}\omega^{-1}Ck_2 \quad [15]$$

were employed.

Typical RRDE results for DMeF, DEF, and DBF are shown in Table II. In the absence of CO_2, $N_k = N$, the theoretical collection efficiency (0.555), for both DEF and DBF. In the presence of CO_2, N_k is appreciably smaller than N for both compounds, showing a significant extent of reaction between the radical anion and dissolved CO_2 on the RRDE time scale. The independence of N_k with concentration and $CONI$ for these two compounds agrees very well with an uncomplicated pseudo-first-order mechanism. Typical results for DMeF are shown in Fig. 2. The slight dependence of N_k on $CONI$, can be attributed to the simultaneous occurrence of the $F^{\cdot-}$ dimerization reaction (12). However, the N_k values are considerably smaller than those under identical conditions but without dissolved CO_2.

The experimental points in Fig. 2 were fit by using the known dimerization parameter, $XKTC$, and adding the pseudo-first-order reaction parameter XKT for k_F. Values of k_{2F} were obtained previously (12); for

Table II. Collection efficiency at the RRDE in CO_2-saturated 0.1M TBAI-DMF solutions

Concentration, C (mM)	Rotation rate (rad/sec)	i_d (μA)	$CONI$ ($i_d/i_{d,1}$)	N_k
		Dimethyl fumarate		
0.83	109	8.6	0.137	0.454
		16.4	0.262	0.455
		27.2	0.434	0.453
		38.5	0.615	0.450
		48.1	0.768	0.449
		57.9	0.925	0.446
0.83	157	10.0	0.132	0.470
		19.4	0.255	0.469
		32.2	0.424	0.466
		45.6	0.600	0.466
		57.2	0.753	0.463
		70.0	0.921	0.462
1.37	109	13.2	0.129	0.426
		40.2	0.394	0.420
		57.5	0.564	0.416
		73.0	0.716	0.416
		85.0	0.833	0.417
		95.8	0.939	0.414
		102.0	1.000	0.412
1.37	157	27.2	0.139	0.445
		44.7	0.360	0.443
		64.9	0.523	0.441
		84.7	0.683	0.438
		109.5	0.883	0.438
		116.0	0.935	0.437
		124.0	1.000	0.435
		Diethyl fumarate		
1.82	157	24.5	0.188	0.522
		57.1	0.439	0.523
		90.1	0.692	0.525
		128	0.983	0.523
3.65	157	44.5	0.176	0.524
		100.3	0.398	0.522
		160	0.635	0.525
		223	0.885	0.524
		252	1.00	0.523
4.87	157	57.5	0.172	0.522
		125.3	0.375	0.524
		199	0.596	0.523
		259	0.775	0.525
		324	0.970	0.522
6.10	157	136	0.328	0.525
		178	0.428	0.522
		260	0.625	0.523
		330	0.793	0.521
		398	0.957	0.522
		Di-n-butyl fumarate		
3.30	157	45.0	0.230	0.531
		99.8	0.510	0.533
		150.5	0.770	0.530
		177.2	0.906	0.529
		195.5	1.00	0.530
1.54	157	34.1	0.372	0.531
		55.2	0.601	0.530
		70.5	0.766	0.533
		92.0	1.000	0.532

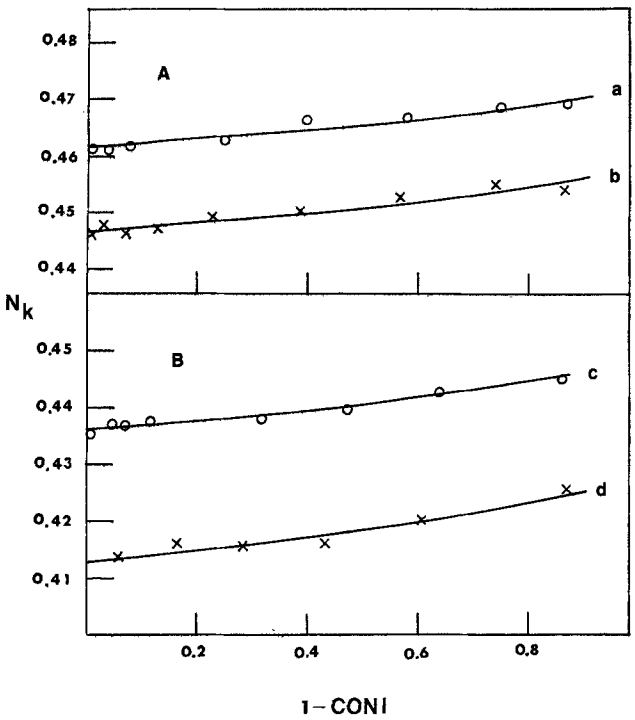

Fig. 2. Collection efficiency (N_k) vs. 1-*CONI* for dimethyl fumarate in presence of CO_2. Experimental points: (x) $\omega = 109$ sec^{-1}, (o) $\omega = 157$ sec^{-1}, (A) 0.83 mM DMeF, (B) 1.37 mM DMeF. Theoretical lines correspond to (a) $XKTC = 0.0086$, $XKT = 0.135$; (b) $XKTC = 0.0127$, $XKT = 0.16$; (c) $XKTC = 0.0144$, $XKT = 0.18$; (d) $XKTC = 0.0208$, $XKT = 0.22$.

DMeF $k_{2F} = 110$ M^{-1} sec^{-1}. $XKTC$ values were calculated for the various concentrations and rotation rates used in this work. For example, line a in Fig. 2 was generated by digital simulation using $XKTC = 0.0127$ and $XKT = 0.16$ for $C = 0.83$ m*M*. These lines fit the experimental points quite well. Values of $XKTC$ for DEF and DBF were negligible compared to XKT. Values of XKT and k_F for these three compounds obtained by this method at different C and ω values are given in Table III. The average values of k_F are DMeF, 1.5, DEF, 0.47, and DBF, 0.35 (sec^{-1}). The fit of the data to this pseudo-first-order mechanism is persuasive evidence for the reaction sequence [13] and [16] with rapid coupling of the $FCO_2^{\cdot-}$

$$2FCO_2^{\cdot-} \rightarrow {}^-O_2CDCO_2^- \qquad [16]$$

In an attempt to detect $FCO_2^{\cdot-}$, several ESR experiments were undertaken. A 10 m*M* DEF solution was reduced with a constant current of 20 μA in a flat cell inside the cavity of the ESR spectrometer. The steady-state spectrum which resulted after about 1 min of electrolysis was essentially the same as those previously reported (20, 25). The spectrum obtained in a saturated CO_2 solution was the same as that from a CO_2-free system. The ESR spectrum of $FCO_2^{\cdot-}$ would be different than that of $F^{\cdot-}$, since the added CO_2 would change the symmetry and the proton hyperfine coupling constants. Hence the $FCO_2^{\cdot-}$ species must be too short-lived to detect by this method. The reaction of $F^{\cdot-}$ and CO_2 can be seen, however, from the time dependence of the spectra (Fig. 3). After steady-state signals were generated, the constant current responsible for generating the radical anion was turned off and the spectrum was recorded immediately at a

Table III. Calculated rate constants for reactions of fumarate radical anions in the presence of CO_2 from RRDE results[a]

Concentration, C (mM)	Rotation rate ω (sec^{-1})	$XKTC$[b]	k_{2F}[b] (M^{-1} sec^{-1})	XKT_F[c]	$(XKT_F)\omega$[c]	k_F (sec^{-1})
			A. Dimethyl fumarate			
0.83	109	0.0127	1.1×10^2	0.16	17.4	1.2
	157	0.0086	1.1×10^2	0.135	21.2	1.4
	207	0.0067	1.1×10^2	0.11	22.8	1.5
1.37	109	0.0208	1.1×10^2	0.22	24.0	1.6
	157	0.0144	1.1×10^2	0.18	28.3	1.9
				Avg	22.7	1.5 ± 0.2
			B. Diethyl fumarate			
1.83	109		44[d]	0.055	5.45	0.41
	157			0.045	7.06	0.47
	207			0.037	7.66	0.51
	257			0.025	6.43	0.43
2.43	109			0.059	6.43	0.43
	157			0.042	6.60	0.44
	207			0.034	7.04	0.47
3.65	109			0.064	6.98	0.46
	157			0.045	7.06	0.47
	207			0.035	7.24	0.48
	257			0.028	7.20	0.48
4.87	109			0.066	7.20	0.48
	157			0.047	7.38	0.49
	207			0.033	6.83	0.46
	257			0.026	6.67	0.45
6.10	109			0.066	7.20	0.48
	157			0.047	7.38	0.49
	207			0.035	7.24	0.48
	257			0.026	6.67	0.45
				Avg	6.93	0.47 ± 0.02
			C. Di-n-butyl fumarate			
1.10	109		26[d]	0.050	5.45	0.36
	157			0.031	4.86	0.32
	207			0.022	4.55	0.30
1.54	109			0.055	6.00	0.40
	157			0.033	5.18	0.35
	207			0.020	4.55	0.28
2.20	109			0.048	5.23	0.35
	157			0.034	5.34	0.36
	207			0.025	5.18	0.35
3.30	109			0.057	6.21	0.41
	157			0.034	5.34	0.36
	207			0.026	5.38	0.36
				Avg	5.27	0.35 ± 0.03

[a] The solutions were all 0.1*M* TBAI in DMF. The RRDE had $r_1 = 0.187$ cm, $r_2 = 0.200$ cm, and $r_3 = 0.332$ cm.
[b] $XKTC$ is digital simulation parameter for dimerization of the anion radicals $2F^{\cdot-} \rightarrow D^{2-}$ with reaction rate constant k_{2F} from Ref. (4).
[c] $XKTF = (0.51)^{-2/3} \nu^{1/3} D^{-1/3} \omega^{-1} k_F$, $\nu = 0.00849$ cm^2/sec for the reaction of the radical anion with saturated CO_2, $F^{\cdot-} + CO_2 \xrightarrow{k_F} FCO_2^{\cdot-}$ as a pseudo-first-order reaction.
[d] Negligible dimerization reaction on the RRDE time scale, data from Ref. (5).

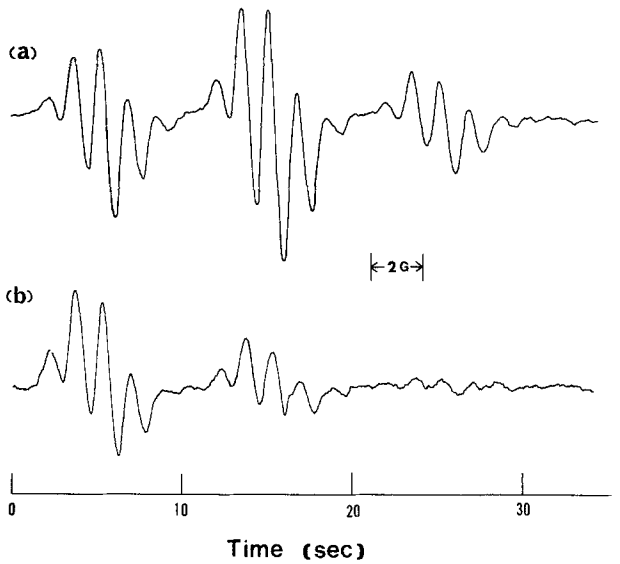

Fig. 3. ESR spectra of 10 mM diethyl fumarate in 0.1M TBAI-DMF electrolyzed at 20 μA in (a) absence and (b) saturated with CO_2. Scan rate 40 G/min.

high scan rate (40 G/min). At this scan rate, good resolution was sacrificed but any differences in signal intensities with time were recorded. In the presence of CO_2 (Fig. 3b) the ESR signals decayed almost to zero 30 sec after the current was turned off. On the other hand, ESR signals still remained reasonably strong in the absence of CO_2 (Fig. 3a) when the generating current was turned off after the same period of time.

Dimethyl maleate (DMM), diethyl maleate (DEM), and di-n-butyl maleate (DBM).—The analysis of the behavior of the maleates parallels that of the fumarates, but is more complicated because of the rapid isomerization and coupling reactions of $M^{\cdot-}$. In the presence of CO_2 the voltammetric reduction waves at the RRDE (at −1.0V *vs.* Ag-RE) are shifted slightly (10-20 mV) toward less negative potentials with essentially no change in the Levich constant (Table I) compared to solutions without CO_2. Variation of N_k with *CONI* [(defined as in (12)] was determined at several values of C and ω; typical results are given in Fig. 4. For determinations of N_k, E_r was adjusted to −0.8V *vs.* Ag-RE, on the plateau of the fumarate reduction wave (where F is reduced to $F^{\cdot-}$ and $M^{\cdot-}$ is oxidized to M). Under these conditions the contribution of $M^{\cdot-}$ oxidation to the ring current can be determined, as discussed previously (12). The N_k values so obtained were used to determine the pseudo-first-order rate constant, k_M (or *XKT*), using the values of k_1 and k_{2M} measured in the absence of CO_2 and digital simulation methods. The solid lines in Fig. 4 are such simulated curves and results for maleates are given in Table IV. Note that carboxylation of $F^{\cdot-}$ (resulting

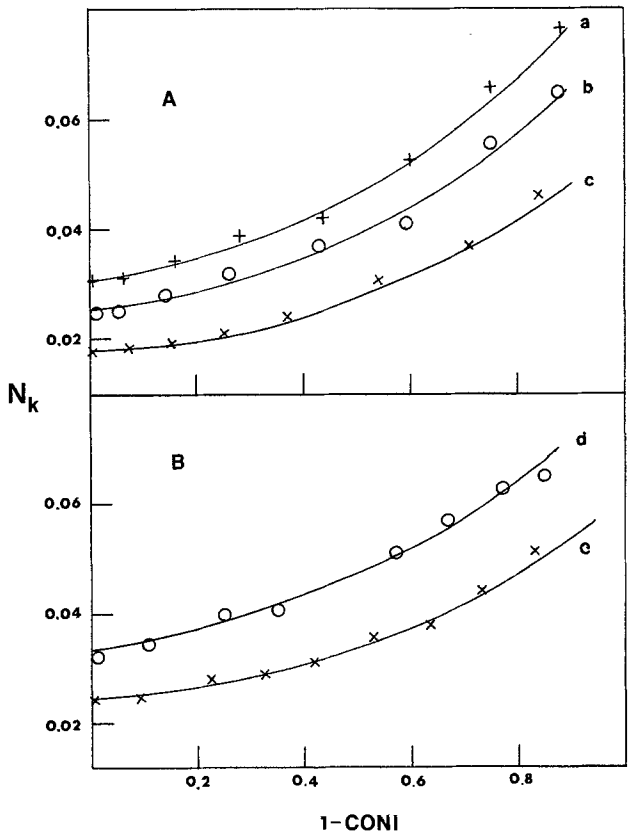

Fig. 4. Collection efficiency (N_k) *vs.* 1-*CONI* for diethyl maleate in presence of CO_2. Experimental points: (x) $\omega = 157$ sec^{-1}, (o) $\omega = 207$ sec^{-1}, (+) $\omega = 257$ sec^{-1}, (A) 2.66 mM DMM, (B) 1.24 mM DMM. Theoretical lines correspond to the following respective values of *XKTC* (dimerization), *XKT* (isomerization), and *XKT* (CO_2 reaction): (a) 12, 0.35, 1.30; (b) 14.9, 0.435, 1.34; (c) 19.7, 0.57, 1.63; (d) 8.16, 0.435, 1.51; (e) 10.8, 0.57, 1.78.

Table IV. Calculated rate constants for reactions of maleate anion radicals in the presence of CO_2 from RRDE results[a]

Concentration, C (mM)	Rotation rate ω (sec^{-1})	$XKTC$[e]	k_{2M}[e] (M^{-1} sec^{-1})	XKT_1[f]	k_1[f] (sec^{-1})	XKT_M[c]	k_M[c] (sec^{-1})
			A. Dimethyl maleate				
0.52	157	9.35	1.88×10^3	0.21	2.2	2.89	30.2
	207	7.1	1.88×10^3	0.16	2.2	2.54	35.0
1.05	157	18.9	1.88×10^3	0.21	2.2	2.79	29.2
	207	14.3	1.88×10^3	0.16	2.2	2.44	33.7
						Avg	32.0 ± 2.8
			B. Diethyl maleate				
1.24	157	10.8	9.1×10^4	0.57	6.0	1.78	18.6
	207	8.16	9.1×10^4	0.435	6.0	1.51	20.8
2.26	157	19.7	9.1×10^4	0.57	6.0	1.63	17.1
	207	14.9	9.1×10^4	0.435	6.0	1.34	18.5
	257	12.0	9.1×10^4	0.35	6.0	1.30	22.2
						Avg	19.4 ± 1.9
			C. Di-n-butyl maleate				
1.97	207	9.90	6.88×10^4	0.48	6.7	1.32	18.2
	257	7.98	6.88×10^4	0.39	6.7	0.96	16.4
2.42	207	12.10	6.88×10^4	0.48	6.7	1.42	19.6
	257	9.75	6.88×10^4	0.39	6.7	1.04	17.7
						Avg	18.0 ± 1.4

[a,c] As defined in the footnote of Table III.
[e] Dimerization of radical anions from Ref. (12).
[f] Isomerization of maleate radical anions to fumarate radical anions from Ref. (12).

from isomerization of $M^{-\cdot}$) does not enter into this calculation, since E_r is such that $F^{-\cdot}$ is not oxidized at the ring, and $FCO_2^{-\cdot}$ is too short-lived to be detected. The values of k_M so calculated are: DMM, 32; DEM, 19; and DBM, 18 (sec^{-1}).

Conclusions

The carboxylation reactions of the *cis-* and *trans-* radical anions in general follow previously reported behavior (12, 13). The reaction rate constants decrease slightly as the alkyl group becomes more bulky, because of steric hindrance. The maleate radical anions are much more reactive toward CO_2 than the corresponding *trans-* species, as has previously been seen for radical ion coupling and for reaction with acrylonitrile. This has been attributed to greater electron density at the central ethylenic carbon atoms because of charge repulsion of the neighboring carbonyl groups.

Acknowledgments

The support of this research by the Robert A. Welch Foundation and the National Science Foundation (CHE 71-03344) is gratefully acknowledged.

Manuscript submitted July 7, 1976; revised manuscript received Sept. 30, 1976.

Any discussion of this paper will appear in a Discussion Section to be published in the December 1977 JOURNAL. All discussions for the December 1977 Discussion Section should be submitted by Aug. 1, 1977.

REFERENCES

1. M. M. Baizer, in "Organic Electrochemistry," M. M. Baizer, Editor, chap. XIX, Marcel Dekker, Inc., New York (1973).
2. J. P. Petrovich, M. M. Baizer, and M. R. Ort, *This Journal*, **116**, 743 (1969).
3. W. V. Childs, J. T. Maloy, C. P. Keszthelyi, and A. J. Bard, *ibid.*, **118**, 874 (1971).
4. V. J. Puglisi and A. J. Bard, *ibid.*, **119**, 829 (1972).
5. M. J. Hazelrigg and A. J. Bard, *ibid.*, **122**, 211 (1975).
6. I. B. Goldberg, D. Boyd, R. Hirasawa, and A. J. Bard, *J. Phys. Chem.*, **78**, 295 (1974).
7. E. Lamy, L. Nadjo, and J. M. Savéant, *J. Electroanal. Chem.*, **42**, 189 (1973).
8. E. Lamy, L. Nadjo, and J. M. Savéant, *ibid.*, **50**, 141 (1974) and numerous references therein.
9. R. D. Grypa and J. T. Maloy, *This Journal*, **122**, 377 (1975).
10. R. D. Grypa and J. T. Maloy, *ibid.*, **122**, 509 (1975).
11. I. Vartires, W. H. Smith, and A. J. Bard, *ibid.*, **122**, 894 (1975).
12. L. S. R. Yeh and A. J. Bard, *ibid.*, **124**, 189 (1977).
13. A. J. Bard, V. J. Puglisi, J. V. Kenkel, and A. Lomax, *Faraday Discuss. Chem. Soc.*, **56**, 353 (1973).
14. S. Wawzonek and A. Gunderson, *This Journal*, **111**, 324 (1964).
15. S. Wawzonek, R. C. Duty, and J. H. Wagenknecht, *ibid.*, **111**, 74 (1964).
16. N. L. Weinberg, A. K. Hoffmann, and T. B. Reddy, *Tetrahedron Lett.*, **1971**, 2271.
17. R. Dietz and M. E. Peover, *Discuss. Faraday Soc.*, **45**, 154 (1968).
18. D. A. Tyssee and M. M. Baizer, *J. Org. Chem.*, **39**, 2819 (1974).
19. D. A. Tyssee and M. M. Baizer, *ibid.*, **39**, 2823 (1974).
20. I. B. Goldberg and A. J. Bard, in "Magnetic Resonance in Chemistry and Biology," J. N. Herak and K. J. Adamic, Editors, p. 297, Marcel Dekker, Inc., New York (1975).
21. H. Stephene and T. Stephene, "Solubility of Inorganic and Organic Compounds," Vol. 1, Part 2, p. 1063, MacMillan Co., New York (1963).
22. J. M. Nigretto and A. J. Bard, *This Journal*, **123**, 1303 (1976).
23. J. P. Petrovich, M. M. Baizer, and M. R. Ort, *ibid.*, **116**, 749 (1969).
24. K. B. Prater and A. J. Bard, *ibid.*, **117**, 1517 (1970) and references therein.
25. S. F. Nelsen and J. P. Gillespie, *J. Org. Chem.*, **40**, 2391 (1975).

The Ag^+-Ag Exchange Reaction in Aqueous Acidic Nitrate Electrolyte

D. Larkin

Department of Chemistry, Towson State University, Towson, Maryland 21204

and N. Hackerman*

Department of Chemistry, Rice University, Houston, Texas 77001

ABSTRACT

The exchange reaction at polycrystalline silver electrodes has been investigated for the system Ag-$AgNO_3$-KNO_3 using a faradaic impedance method. The exchange reaction was determined to be adatom diffusion controlled and the exchange current was found to be dependent on *p*H. It is suggested that H_3O^+ inhibits the exchange reaction through an adsorption process which blocks the crystal growth sites.

Few investigations have been made of the exchange mechanism for the system

$$Ag^+_{(soln)} + e \rightleftharpoons Ag_{(s)} \qquad [1]$$

in aqueous solutions. This is surprising as silver would not be expected to suffer, to the same degree, from the formation of oxide or hydroxide films on the electrode surface as do many other more extensively studied metals, *i.e.*, the exchange reaction should not be complicated by the possibility of chemical and electrochemical reactions of the type

$$M(H_2O)^{n+}{}_{y(soln)} \rightleftharpoons M(H_2O)^{n+}{}_{y(ads)}$$

$$M(H_2O)^{n+}{}_{y(ads)} \rightleftharpoons M(OH)_n + nH_3O^+ \qquad [2]$$

$$M(OH)_{n(ads)} + ne \rightleftharpoons M_{(solid)} + nOH^-_{(soln)}$$

The absence of a surface oxide or hydroxide film is further indicated by the large polarizable region exhibited by silver (1) [~0.5 to −1.1V (NHE)]. This

* Electrochemical Society Active Member.